Special Issue Article

Advances in Mechanical Engineering

Advances in Mechanical Engineering
2018, Vol. 10(1) 1–10
© The Author(s) 2018
DOI: 10.1177/1687814017740710
journals.sagepub.com/home/ade
SAGE

A universal algorithm for sensorless collision detection of robot actuator faults

Saixuan Chen[1], Minzhou Luo[1,2,3] and Feng He[2]

Abstract

When a robot is working properly, it is possible to collide with people or objects entering its working space. This research is different than usual control algorithm. It proposes a universal algorithm for sensorless collision detection of robot actuator faults to enhance the security of the robot. On the basis of the dynamic model, a classical friction model to ensure the accuracy of the whole dynamic model is introduced. This collision detection algorithm can conduct without any external sensors or acceleration and realize the real-time detection just needs to measure the motor current and the location information from the encoder of the robot joint. The value of external torque τ_{ext} was used to compare with the threshold to detect the collision. After using the proposed collision detection method, the two rotational (2R) planar manipulators can detect the slight collision reliably. The experimental results and performance comparisons show that this sensorless collision detection algorithm is simple and effective. It can be promoted to any other type of robot arm with more degrees of freedom.

Keywords

Dynamic, sensorless collision detection, friction torque model, motor current, residual error

Date received: 30 July 2017; accepted: 10 October 2017

Handling Editor: Fei Chen

Introduction

For obtaining a compliant flexible design of robot which has the capability of interacting and collaborating with human, it should fulfill some parameters to achieve this task. These robots should be flexible and compliant to achieve the collaboration and interaction feature. This feature needs some consideration in the mechanical structure design of the robot and the choosing of hardware devices. The most important side is implementing complex control techniques. We will refer to some of the recent research work and techniques for both mechanical design and control side. And in the top of all these parameters, we need to consider the safety issues. Safety should be the dominant parameter for such robots design.

For achieving this, we need to utilize actuators which are capable of modulating torque and impedance (stiffness and/or damping) simultaneously, continuously, and independently.[1] There is some research work in that direction. Automatic collision avoidance is achieved by the control design at the kinematic level exploiting the joint space redundancy.[2,3] The variable impedance actuators (VIA),

[1]School of Engineering Science, University of Science and Technology of China, Hefei, China
[2]Institute of Intelligent Manufacturing Technology, Jiangsu Industrial Technology Research Institute, Nanjing, China
[3]Key Laboratory of Special Robot Technology of Jiangsu Province, Hohai University, Changzhou, China

Corresponding author:
Minzhou Luo, School of Engineering Science, University of Science and Technology of China, No. 96, JinZhai Road Baohe District, Hefei 230026, China.
Email: luomz@iimt.org.cn

series-elastic actuators (SEAs),[4] and variable-stiffness actuators (VSAs)[5] were used in these researches. In Qiu et al.,[6] they combine vision compressive sensing, brain–machine reference commands, and adaptive fuzzy control to develop a teleportation control system for exoskeleton robots. Moreover, harmonic drives could be utilized for this task. These actuators can reach the required features of the robot but on the most important side, it needs complex control strategies.

How to enhance the security of the industry robot can begin at collision detection. There are some researches about it and some researchers acquired certain results. The most effective, fast, and simplest method of detecting the collision of the robot is adding external sensor.[7–9] Although this method can detect the collision force accurately, it can just detect the place and the high-precision sensors are expensive. There are fewer companies that can afford so high price sensors equipped on the robots. Phan et al.[10] introduced an internal sensor measurement method. It captures the torques of each joint and the values of each encoder. The driving moment of the robot in the motion can be calculated by the dynamic model. Comparing the calculated torque and the captured torque, the collision can be detected. This method needs to calculate the first and second derivatives of the position. This process may lead to the noise and will affect the accuracy of the system. Yamada et al.[11] and De Luca and Mattone[12] introduced a detection method based on the kinetic momentum. This method regards the collision as the system fault. It can detect the collision perfectly, but it has some interaction effects on timeliness and accuracy of tracking the external force. It is hard to have good timeliness and accuracy simultaneity. There are also other detection collision/interaction techniques without using external sensors, such as in De Luca and colleagues.[13,14]

The sensorless collision detection is the latest research direction. This technique does not use any extra sensors, such as torque sensors or accelerometers, and it is proposed in this research. A dynamic model and a friction model of the robot joints are also developed for this purpose. This research can realize the real-time detection just needs to measure the motor current and the location information from the encoder of the robot joint. The observed value of residual error was used to compare with the threshold to detect the collision. In order to verify the accuracy of the algorithm of collision detection method, a $2R$ planar manipulator was built. We made some experiments on it. The experimental results show that the collision can be detected reliably and the manipulator can stop immediately when the collision occurs.

Collision and interaction detection

For the robot to be able to collaborate with humans physically, there should be a technique with certain control strategy to detect the physical collisions and interactions. This research realizes the real-time detection just needs to measure the motor current and the location information from the encoder of the robot joint. The observed value of residual error was used to compare with the threshold to detect the collision.

Rigid body dynamic model

The dynamic model of robot mechanism can be described as

$$\mathbf{M}(\mathbf{q})\ddot{\mathbf{q}} + \mathbf{c}(\mathbf{q}, \dot{\mathbf{q}})\dot{\mathbf{q}} + \mathbf{g}(\mathbf{q}) = \boldsymbol{\tau}_{tot} \tag{1}$$

$\mathbf{q}$ is the generalized coordinate vector of the robot. $\dot{\mathbf{q}}$ and $\ddot{\mathbf{q}}$ replace the velocity and acceleration of each joint, respectively. $\mathbf{M}$(q) is an inertia matrix of the robot and it is also a positive-definite matrix. $\mathbf{c}(\mathbf{q}, \dot{\mathbf{q}})$ is the Coriolis matrix of the robot. The vector $\mathbf{c}(\mathbf{q}, \dot{\mathbf{q}})\dot{\mathbf{q}}$ contains Coriolis force and Centrifugal force. $\mathbf{g}(\mathbf{q})$ is the gravitation vector act on each joint. $\boldsymbol{\tau}_{tot}$ is the sum of all joint torques (rotational joints). When there is no friction and other external torques acting on the robot, $\boldsymbol{\tau}_{tot}$ is just the motor torque.[15]

When a robot is working properly, it is possible to collide with people or objects entering its working space. Then the dynamics equation is

$$\mathbf{M}(\mathbf{q})\ddot{\mathbf{q}} + \mathbf{c}(\mathbf{q}, \dot{\mathbf{q}})\dot{\mathbf{q}} + \mathbf{g}(\mathbf{q}) = \boldsymbol{\tau}_j - \boldsymbol{\tau}_{ext} \tag{2}$$

1. The dynamical parameters of each joint can be calculated from the computer-aided design (CAD) data after added the materials on the robot. The position vector $\mathbf{q}$ can be measured by the magnetic encoders of the robot joint. The velocity vector $\dot{\mathbf{q}}$ and acceleration vector $\ddot{\mathbf{q}}$ can be calculated by the position vector $\mathbf{q}$ through taking the derivative of the time.
2. The joint torque $\boldsymbol{\tau}_j$ can be calculated through the motor torque $\boldsymbol{\tau}_m$ and joint friction torque $\boldsymbol{\tau}_f$ (This will be explained in details in the section "Estimation of the joint torque").

There are many types of research on the acceleration value $\ddot{q}$ before. The acceleration $\ddot{q}$ can be measured directly using the accelerometer as represented in Lee et al.[16] and Axelsson et al.[17] Other methods are combining the accelerometer with a gyroscope when the accelerometer cannot provide useful information in case that the rotation axis is parallel to the direction of gravity.[18,19]

By monitoring the external torque τ_e, collisions can be detected. However, equation (2) cannot be directly

used to compute τ_e, since the acceleration value $\ddot{q}$ is hard to obtain. In this research, $\ddot{q}$ can be solved systematically using an observer based on the generalized momentum equation.

The dynamic model based on the generalized momentum

The generalized momentum of the robot can be defined as

$$\mathbf{p} = \mathbf{M}(\mathbf{q})\dot{\mathbf{q}} \tag{3}$$

This equation (3) satisfies the first-order equation by taking the derivative of $\mathbf{p}$, we can find

$$\dot{\mathbf{p}} = \mathbf{M}(\mathbf{q})\ddot{\mathbf{q}} + \dot{\mathbf{M}}(\mathbf{q})\dot{\mathbf{q}} \tag{4}$$

Knowing that $\mathbf{c}(\mathbf{q}, \dot{\mathbf{q}})$ is the Coriolis matrix of the robot. It contains Coriolis and centrifugal

$$\mathbf{c}(\mathbf{q}, \dot{\mathbf{q}}) = \dot{\mathbf{M}}(\mathbf{q})\dot{\mathbf{q}} - \frac{1}{2}\left[\dot{\mathbf{q}}^T \frac{\delta \mathbf{M}(\mathbf{q})}{\delta q_i}\dot{\mathbf{q}}\right] \tag{5}$$

The dynamic model can be represented as

$$\underbrace{\mathbf{M}(\mathbf{q})\ddot{\mathbf{q}} + \dot{\mathbf{M}}(\mathbf{q})\dot{\mathbf{q}}}_{\dot{\mathbf{p}}} \underbrace{- \frac{1}{2}\left[\dot{\mathbf{q}}^T \frac{\delta \mathbf{M}(\mathbf{q})}{\delta q_i}\dot{\mathbf{q}}\right] + \mathbf{g}(\mathbf{q})}_{\boldsymbol{\alpha}(\mathbf{q}, \dot{\mathbf{q}})} = \boldsymbol{\tau}_j - \boldsymbol{\tau}_{ext} \tag{6}$$

where the components $\boldsymbol{\alpha}(\mathbf{q}, \dot{\mathbf{q}})$ can be defined as[20]

$$\boldsymbol{\alpha}(\mathbf{q}, \dot{\mathbf{q}}) = \mathbf{g}(\mathbf{q}) - \frac{1}{2}\dot{\mathbf{q}}^T \frac{\delta \mathbf{M}(\mathbf{q})}{\delta q_i}\dot{\mathbf{q}} \ (i = 1, \ldots, n) \tag{7}$$

Rearranging equation (6), the new dynamic model can be obtained as

$$\dot{\mathbf{p}} + \boldsymbol{\alpha}(\mathbf{q}, \dot{\mathbf{q}}) = \boldsymbol{\tau}_j - \boldsymbol{\tau}_{ext} \tag{8}$$

Estimation of the joint torque

In this research, the joint torque based on the motor torque is generally connected with the motor input current. The joint torque $\boldsymbol{\tau}_j$ can be calculated using the motor torque $\boldsymbol{\tau}_m$ and joint friction torque $\boldsymbol{\tau}_f$. In general, the robot joint meets the standard of common robot design practices. It consists of a motor, a harmonic driver, and an output to the joint. The collaborative robot joint is shown in Figure 1, what is one joint of our next work about 6-degrees of freedom (DOFs) collaborative robot.

As we know, the motor torque $\boldsymbol{\tau}_m$ is proportional to the motor current $\mathbf{i}_m$

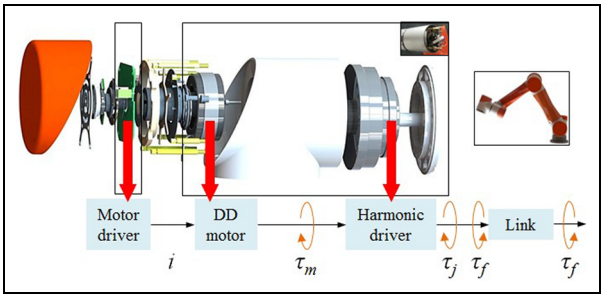

Figure 1. The transmission of the collaborative robot joint.

$$\boldsymbol{\tau}_m = T_c \cdot \mathbf{i}_m \tag{9}$$

T_c is the motor torque constant, which can be got in the motor manual. $n\boldsymbol{\tau}_m$ represents the driving torque of the harmonic drive. The joint torque $\boldsymbol{\tau}_j$ can be calculated by the following equation

$$\boldsymbol{\tau}_j = n\boldsymbol{\tau}_m - \boldsymbol{\tau}_f = n \cdot T_c \cdot \mathbf{i}_m - \boldsymbol{\tau}_f \tag{10}$$

where n is the speed reduction ratio and $\boldsymbol{\tau}_f$ contains three main frictions such as the static friction, the Coulomb friction, and the viscous friction. The friction torque loss in the harmonic drive gear train is the biggest part of the robot. Rearranging equation (8), the new dynamic model can be got as

$$\dot{\mathbf{p}} = n \cdot Tc \cdot \mathbf{i}_m - \boldsymbol{\tau}_f - \boldsymbol{\tau}_{ext} - \boldsymbol{\alpha}(\mathbf{q}, \dot{\mathbf{q}}) \tag{11}$$

where $\mathbf{r} = \boldsymbol{\tau}_{ext} + \boldsymbol{\tau}_f$ contains the terms of external collision torque and the friction torque that should be observed

$$\dot{\mathbf{p}} = n \cdot Tc \cdot \mathbf{i}_m - \mathbf{r} - \boldsymbol{\alpha}(\mathbf{q}, \dot{\mathbf{q}}) \tag{12}$$

Defining the residual error

By calculating the residual of the joint torque, it will be easy to detect the variation which might happen in the joints due to interaction or collision.

Defining the residual $\mathbf{r} = \boldsymbol{\tau}_{ext} + \boldsymbol{\tau}_f$, now we can design the estimator as follows

$$\dot{\hat{\mathbf{r}}} = K(\mathbf{r} - \hat{\mathbf{r}}) \tag{13}$$

We can estimate vector $\mathbf{r}$ as $\hat{\mathbf{r}}$. K is the gain of this estimator. Making the integral of equation (13), we can get the $\hat{\mathbf{r}}(t)$ as

$$\hat{\mathbf{r}}(t) = K\left[\int_0^t (\mathbf{r} - \hat{\mathbf{r}})dt\right] \tag{14}$$

The residual $\mathbf{r} = \boldsymbol{\tau}_{ext} + \boldsymbol{\tau}_f = n \cdot Tc \cdot \mathbf{i}_m - \boldsymbol{\alpha} - \dot{\mathbf{p}}$. Rearranging equation (14), the new $\hat{\mathbf{r}}(t)$ can be got as

$$\hat{\mathbf{r}}(t) = K\left[\int_0^t (n \cdot Tc \cdot \mathbf{i}_m - \boldsymbol{\alpha} - \hat{\mathbf{r}})dt - \mathbf{p}\right]$$
$$= K\left[\int_0^t \left(n \cdot Tc \cdot \mathbf{i}_m + \frac{1}{2}\dot{\mathbf{q}}^T \frac{\delta M(q)}{\delta q}\dot{\mathbf{q}} - \mathbf{g}(\mathbf{q}) - \hat{\mathbf{r}}\right)dt - \mathbf{p}\right] \quad (15)$$

where the position vector $\mathbf{q}$ and velocity vector $\dot{\mathbf{q}}$ can be measured by the photoelectric encoders of the motors. $\hat{r}(t)$ is the observed value of $r(t)$. The initial condition of this system can be defined as $\hat{r}(0) = 0$. When we set the gain value as $K = 10$,[21] a reasonable response time can be achieved. After assuming that $\hat{\mathbf{r}} = \mathbf{r}$, observing $\mathbf{r}$ without any extra equipment can be achieved.

We can estimate $\boldsymbol{\tau}_{ext}$ from $\hat{\mathbf{r}}(t)$ if $\boldsymbol{\tau}_f$ was given. Because we have assumed that $\hat{\mathbf{r}} = \mathbf{r}$, so $\hat{\mathbf{r}} \approx \boldsymbol{\tau}_{ext} + \boldsymbol{\tau}_f$. Now, how to get the friction torque $\boldsymbol{\tau}_f$ becomes a new difficult problem. The using of force–torque sensor is a good choice, but it is so expensive and many robots will not equip it. Therefore, this research makes the friction model to calculate the value of $\boldsymbol{\tau}_f$ and verifies this method by the experiments.

Friction model for the joint

Friction is a complex nonlinear physical phenomenon, occurs between the contacting surfaces of two objects with relative motions. The friction occurs in all of the mechanical systems and has important effects on the performance. Now, due to the friction with the highly nonlinear characteristic, it often leads to steady-state error, limits cycle, and reduces the performance indexes of the system. In this research, we consider three main frictions. The static friction τ_s describes with the no relative motion but with the trend of relative motion. In general, when an external force τ_e is less than the maximum static friction force τ_s, the static friction force will equal to the external force τ_e, but with the opposite direction. When the external force τ_e is equal to or greater than the maximum static friction force τ_s, the static friction force will equal to the maximum static friction force τ_s, the direction is different to the external force. Then, the friction τ_f can be described as

$$\tau_f = \begin{cases} \tau_e & \text{if } v = 0 \text{ and } |\tau_e| < \tau_s \\ \tau_s \ \mathrm{sgn}(v) & \text{if } v = 0 \text{ and } |\tau_e| \geq \tau_s \end{cases} \quad (16)$$

The Coulomb friction τ_c is proportional to the normal load τ_N, with the opposite direction and does not depend on the area of contact, $\tau_c = \mu_c \cdot \tau_N \cdot \mathrm{sgn}(v)$. μ_c is the Coulomb friction coefficient. The viscous friction τ_v is proportional to the motion velocity, $\tau_v = \mu_v \cdot v$. μ_v is the viscous friction coefficient. In general, the Coulomb friction torque model can combine with viscous friction model, like that $\tau_f = \mu_v \cdot v + \mu_c \cdot \tau_N \cdot \mathrm{sgn}(v)$. Consequently, the friction model for sensorless collision detection can be described by[14]

$$\tau_f = \begin{cases} \tau_e & \text{if } v = 0 \text{ and } |\tau_e| > \tau_s \\ \tau_s \ \mathrm{sgn}(v) & \text{if } v = 0 \text{ and } |\tau_e| \geq \tau_s \\ \mu_v \cdot v + \mu_c \cdot \tau_N \cdot \mathrm{sgn}(v) & \text{otherwise} \end{cases} \quad (17)$$

Current measured through Hall Effect sensor

The motor current should be measured, as to be able to estimate the robot joints torque without using external force/torque sensor. There are few techniques used for measuring the current flow. In this research, we propose using a Hall Effect sensor.

A current-carrying conductor is placed in two different fields. One is the no magnetic field and another is the magnetic field as shown in Figure 2(a) and (b). We can see some difference in electric potential. It will be perpendicular to the magnetic field and the direction of current flow. The Hall Effect sensor can measure the large currents with low power dissipation.

When a robot detects the collision, it must perform an appropriate reaction to minimize the impact. In this research, we propose a reaction strategy for the collision conditions as shown in Figure 2(c).

Embedded system control architecture

The robotics control architecture design nowadays tends to be based on embedded systems in many applications. The embedded systems real-time capabilities made the reliable system to be utilized in most of the robotics applications. There are some limitations for the commercial robotics control systems. The commercial software is usually sold with the hardware. Most of these products just have the applications on position control. Lacking alternative extensibilities make it difficult to suit of our method. Therefore, it is impossible to extend the functionality of the robot. For these reasons, we propose a real-time embedded system based on the open source.

The proposed hardware control system design is shown in Figure 3, and the system hardware consists of the following.

Field programmable gate array

Flexible hardware such as field programmable gate array (FPGA) is currently considered an appropriate solution to increase control performance.[22] Due to its re-programmability, FPGA technology combines low-cost development with a rising integration density[23] making it well highly suitable for embedded systems.

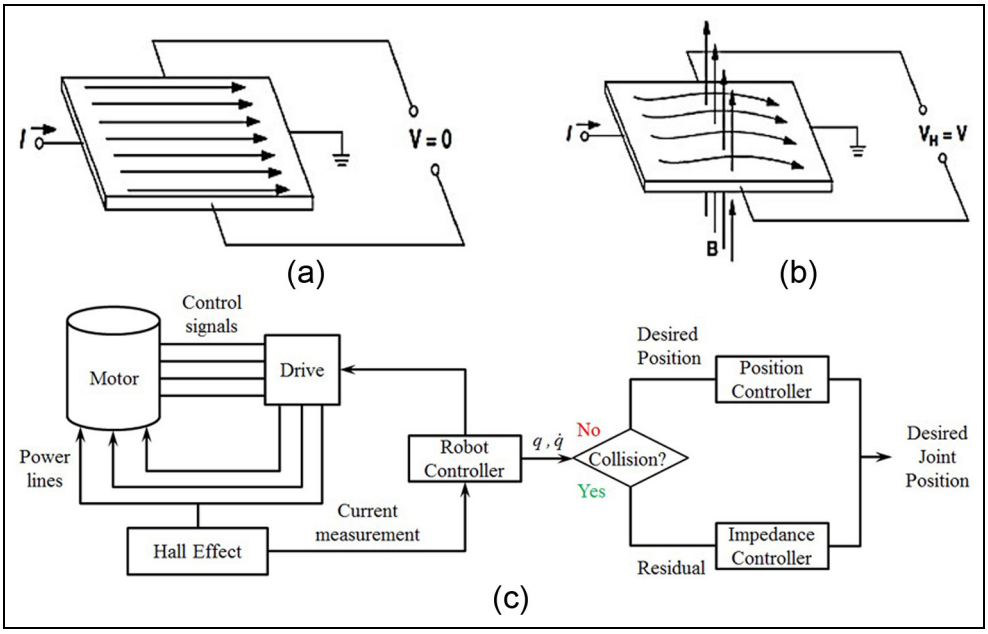

Figure 2. Block diagram for Hall Effect principle and collision reaction strategy: (a) no magnetic field, (b) magnetic field, and (c) collision reaction strategy.

The success is a natural consequence of cost reduction, low power consumption, reliability, real-time characteristic, and significant control performance improvement by dedicated parallel computations.[24,25]

The FPGA is used in our system as a primary robot control system. This controller is responsible for handling all the control routines and algorithms which need real-time capability such as,

- Acquiring the robot internal parameter;
- Executing the trajectory algorithm for his current process;
- Detecting contact/collision;
- Executing collision/obstacle avoidance algorithms;
- Executing human–robot collaboration mode algorithm.

Advanced reduced instruction set computing machines

Advanced reduced instruction set computing (RISC) machines (ARM) is a high-performance embedded processor. It can operate in real time using Linux operating system. The ARM in our proposed system is utilized in the main controller. The block diagram for hardware design is shown in Figure 3.

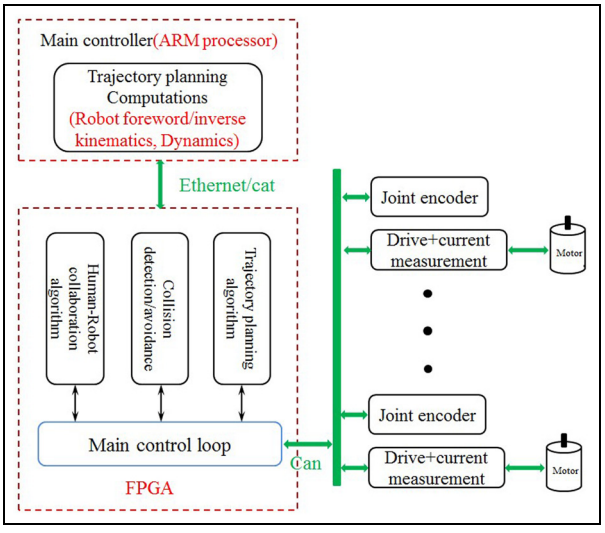

Figure 3. Block diagram for hardware design.

Experimental results

The verification of dynamic model and friction model

In order to verify the accuracy of the dynamic model and the friction model, this research uses the 2*R* planar manipulator to conduct the experiment in Figure 4. This arm was developed just to make experiments for this algorithm in our laboratory. The joint 1 uses the Maxon motor EC45 (70 W) and the harmonic driver CSF-14-100(ratio 100). The joint 2 uses the Maxon motor EC45(50 W) and the harmonic driver CSF-11-100(ratio 100). The whole arm weighs about 4 kg with a payload about 7 kg. The mass of links 1 and 2 was 0.359 and 0.883 kg, respectively. The mass of the joints 1 and 2 was 0.52 and 0.32 kg, respectively. These parameters were needed in the next dynamic model and experiment.

The complicated dynamic model can be got through the Lagrangian with the simplest form. The kinetic energy and potential energy of link 1 and link 2 were

Link 1

$$K_1 = \frac{1}{2}m_1 v_1^2 = \frac{1}{2}m_1 d_1^2 \dot{q}_1^2$$
$$P_1 = m_1 g h_1 = -m_1 g d_1 \cos q_1 \tag{18}$$

Link 2

$$K_2 = \frac{1}{2}m_2 v_2^2 = \frac{1}{2}m_2 \left[d_1^2\dot{q}_1^2 + d_2^2(\dot{q}_1^2 + 2\dot{q}_1\dot{q}_2 + \dot{q}_2^2) + 2d_1 d_2 \cos q_2(\dot{q}_1^2 + \dot{q}_1\dot{q}_2)\right]$$
$$P_2 = -m_2 g d_1 \cos q_1 - m_2 g d_2 \cos(q_1 + q_2) \tag{19}$$

The dynamic equation $L = T - P$ can be calculated through the Lagrangian. Substituting equations (18) and (19) into $L = T - P$, we can get the joint torque T_1 and T_2 for each joint of the arm

$$\begin{aligned} T_1 &= \frac{d}{dt}\frac{\partial L}{\partial \dot{q}_1} - \frac{\partial L}{\partial q_1} \\ &= \left[(m_1 + m_2)d_1^2 + m_2 d_2^2 + 2m_2 d_1 d_2 \cos q_2\right]\ddot{q}_1 \\ &+ \left(m_2 d_2^2 + m_2 d_1 d_2 \cos\theta_2\right)\ddot{q}_2 - 2m_2 d_1 d_2 \sin q_2 \dot{q}_1 \dot{q}_2 \\ &- m_2 d_1 d_2 \sin q_2 \dot{q}_2^2 + (m_1 + m_2) g d_1 \sin q_1 \\ &+ m_2 g d_2 \sin(q_1 + q_2) \end{aligned} \tag{20}$$

$$\begin{aligned} T_2 &= \frac{d}{dt}\frac{\partial L}{\partial \dot{q}_2} - \frac{\partial L}{\partial q_2} \\ &= \left(m_2 d_2^2 + m_2 d_1 d_2 \cos q_2\right)\ddot{q}_1 + m_2 d_2^2 \ddot{q}_2 \\ &+ m_2 d_1 d_2 \sin q_2 \dot{q}_1^2 + m_2 g d_2 \sin(q_1 + q_2) \end{aligned} \tag{21}$$

Rearranging equations (20) and (21), the new matrix of the two links can be got as

$$\begin{bmatrix} T_1 \\ T_2 \end{bmatrix} = \underbrace{\begin{bmatrix} M_{11} & M_{12} \\ M_{21} & M_{22} \end{bmatrix}\begin{bmatrix} \ddot{q}_1 \\ \ddot{q}_2 \end{bmatrix}}_{M(q)\ddot{q}} + \underbrace{\begin{bmatrix} C_{11} & C_{12} \\ C_{21} & C_{22} \end{bmatrix}\begin{bmatrix} \dot{q}_1^2 \\ \dot{q}_2^2 \end{bmatrix} + \begin{bmatrix} B_{11} & B_{12} \\ B_{21} & B_{22} \end{bmatrix}\begin{bmatrix} \dot{q}_1\dot{q}_2 \\ \dot{q}_2\dot{q}_1 \end{bmatrix}}_{c(q,\dot{q})\dot{q}} + \underbrace{\begin{bmatrix} G_1 \\ G_2 \end{bmatrix}}_{g(q)} \tag{22}$$

When the system need not consider the friction, the dynamic model can adopt equation (22). We can get the currents calculated by the dynamic model and measured by the encoder of the motor of the same joint. Comparing the currents, we can get the errors of each joint as Figure 3 shows.

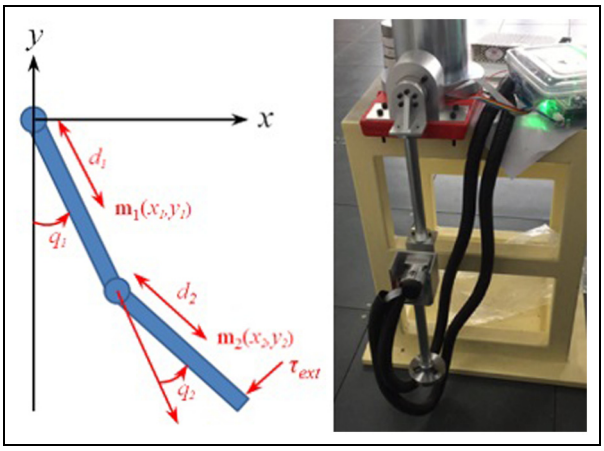

Figure 4. 2*R* planar manipulator.

As Figure 5 shows, the calculated current by the dynamic model and the measured current by the encoder of the motor are the same but have some big errors. The biggest error of joint 1 is 1.5 A and joint 2 is 1.4 A. Such a big error will have a significant impact on subsequent collision detection.

Normally, there are many noises of the mechanical drive system in motion. These will cause low transmission efficiency and cannot get the accuracy dynamic model. According to the previous analysis, this error is caused by the friction mostly. After adding the friction model in the dynamic model (22), the calculated current by the dynamic model and the measured current by the encoder of the motor will become more close as shown in Figure 4.

We can see from the experimental data (shown in Figure 6) that the error of each joint becomes smaller. The biggest error of joint 1 is 1 A and joint 2 is 0.8 A. So, the accuracy of the friction model has the direct bearing on the error.

The accuracy of the dynamic model and the friction model has the direct bearing on the setting of the collision current threshold of collision detection algorithm. So, it is important for the collision detection to correct and identify the error.

Sensorless collision detection

In order to get the experimental result of the sensorless collision detection algorithm, this research uses the 2*R* planar manipulator to conduct the collision detection experiment. The experimental performance and the corresponding results are shown in Figure 7. There is a contrast experiment, one with no collision detection and another one with the collision detection. The

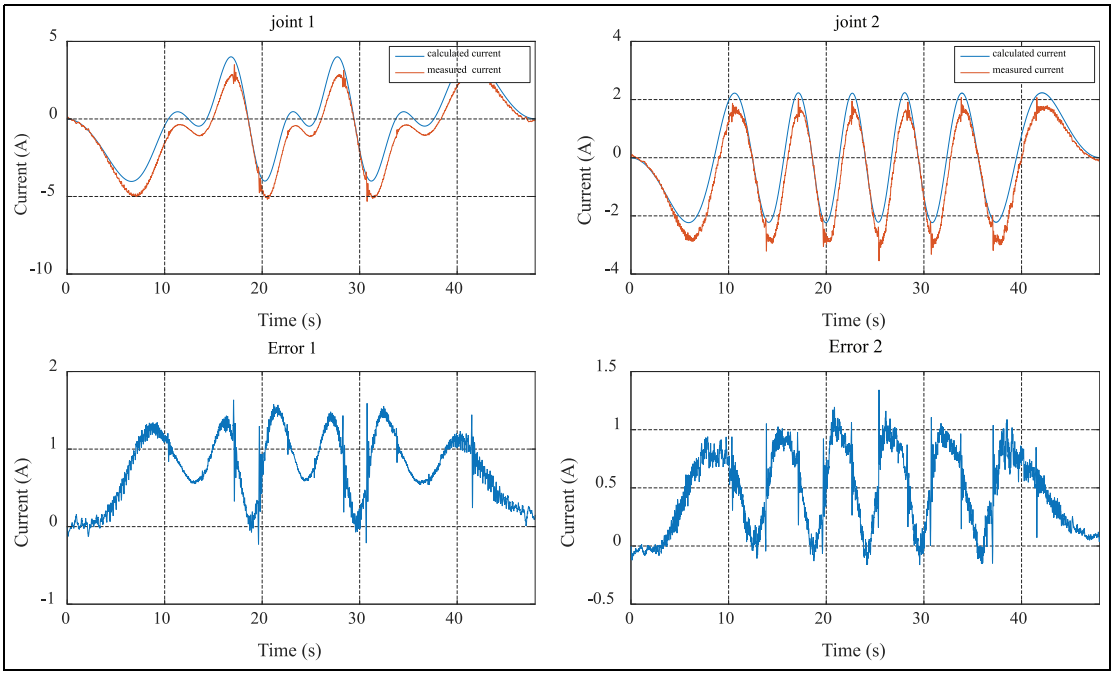

Figure 5. The calculated current and the measured current (no friction model).

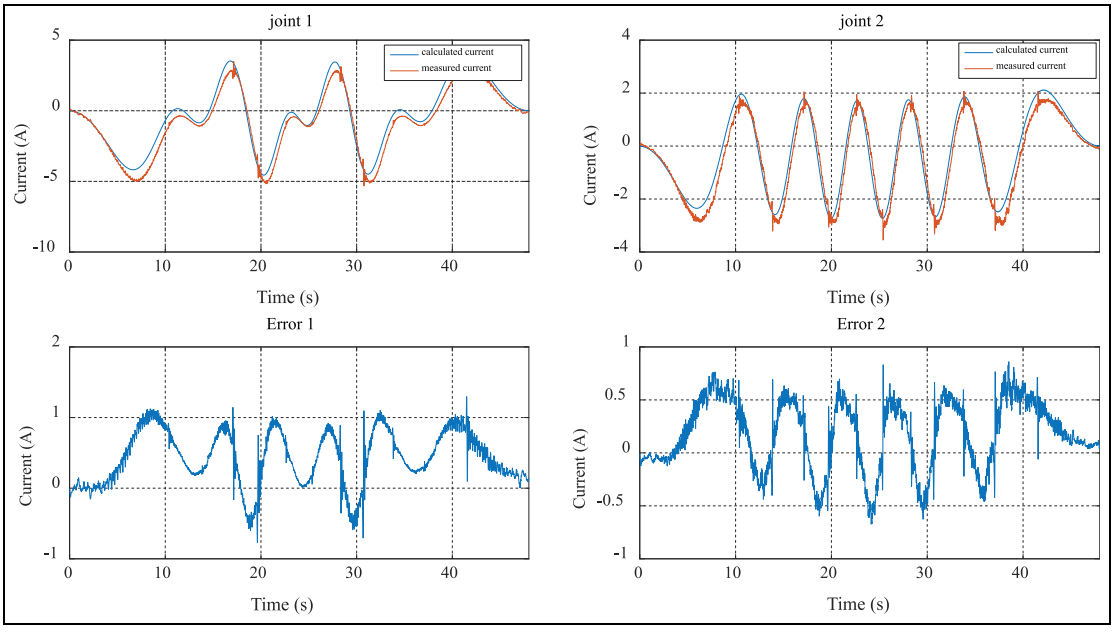

Figure 6. The calculated current and the measured current (add friction model).

experiment uses one paper to collide the arm. Figure 7(a) with no collision detection shows that the paper is broken by the arm. Figure 7(b) with the collision detection shows that the arm stops when it collides with the paper. The data of $\hat{r}(t)$ can be acquired by these experiments.

On the basis of the collision detection algorithm, when the link collided with the paper, the system will detect the collision and the current peak will exceed the threshold. Then, the arm will stop and move back base on the zero gravity. This experiment aims to show the importance of the collision detection algorithm during the instant of the collision.

Figure 8 shows the $\hat{r}(t)$ of joint 2, where the collision was detected at first. Whether the collision happens or not, it can be judged by comparing the absolute value

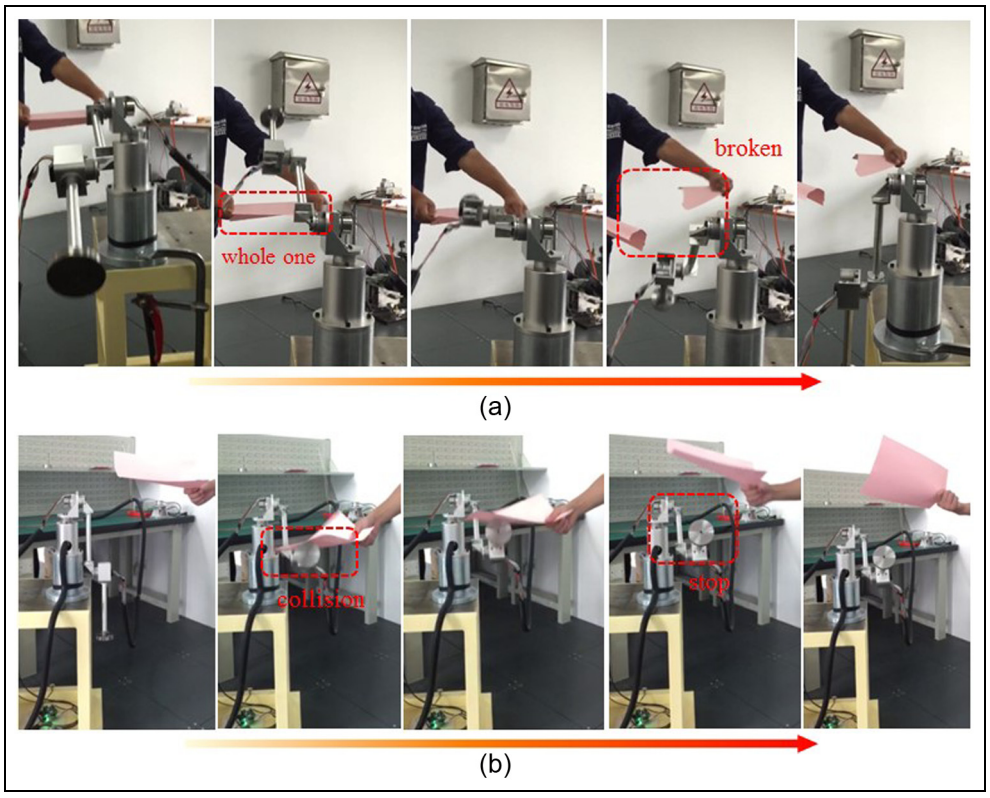

Figure 7. Two experiments: (a) no collision detection and (b) collision detection.

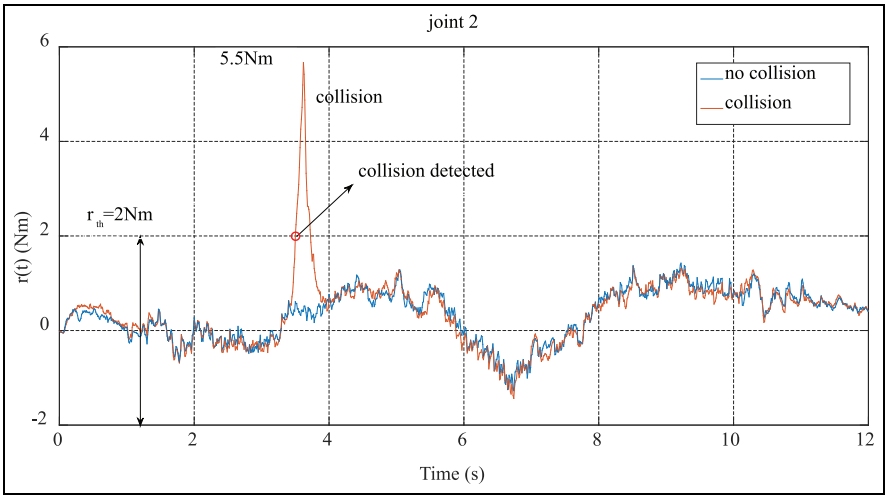

Figure 8. Experimental verification of applicability of sensorless collision detection.

of $\hat{r}(t)$ with a threshold r_{th}. The threshold r_{th} can be determined through the experiments. In this research, we set the threshold r_{th} as 2 N m according to the maximum value of $\hat{r}(t)$ when there is no collision. When a collision takes place, $\hat{r}(t)$ will exceed the threshold r_{th}. This leads to a conclusion that collisions can be detected by checking whether or not $\hat{r}(t)$ exceeds r_{th}.

Conclusion

This research proposes a method about sensorless collision detection algorithm. The friction model is introduced into the dynamic model to enhance the accuracy of the algorithm. The observed value of residual error was used to compare with the threshold to detect the collision. The performance of the proposed collision

detection method was evaluated using a $2R$ planar manipulator. The experimental results show that collision can be reliably detected without any extra sensors. Two important conclusions were summarized:

1. The collision detection algorithm is based on the dynamic model and friction model and no need of extra sensors. Therefore, this method can apply to any industry robot and no need to change the structures of it.
2. The accuracy of the collision detection algorithm depends most on the model of the dynamic and the friction. So establishing a more precise model for the robot is a most important part of the collaborative robot.

There is much research work to do in the future. This collision detection algorithm is just verified on the two-link robot arm. When the 6-DOF collaborative robot is finished, it has a broader application prospects.

Declaration of conflicting interests

The author(s) declared no potential conflicts of interest with respect to the research, authorship, and/or publication of this article.

Funding

The author(s) disclosed receipt of the following financial support for the research, authorship, and/or publication of this article: This work was supported by National Nature Science Foundation of China (No. 51405469).

References

1. Braun D, Petit F, Huber F, et al. Robots driven by compliant actuators: optimal control under actuation constraints. *IEEE T Robot* 2013; 29: 1085–1101.
2. Yang C, Wang X, Cheng L, et al. Neural-learning-based telerobot control with guaranteed performance. *IEEE T Cybernetics* 2017; 47: 3148–3159.
3. Yang C, Wang X, Li Z, et al. Teleoperation control based on combination of wave variable and neural networks. *IEEE T Syst Man Cy: S* 2017; 47: 2125–2136.
4. Pratt G and Williamson M. Series elastic actuators. In: *Proceedings of the international conference on intelligent robots and systems*, Pittsburgh, PA, 5–9 August 1995, pp.399–406. New York: IEEE.
5. Van Ham R, Sugar T, Vanderborght B, et al. Compliant actuator designs. *IEEE Robot Autom Mag* 2009; 16: 81–94.
6. Qiu S, Li Z, He W, et al. Teleoperation control of an exoskeleton robot using brain machine interface and visual compressive sensing. In: *Proceedings of the IEEE transactions on fuzzy systems*, Guilin, China, 12–15 June 2013. New York: IEEE.
7. Lu S, Chung JH and Velinsky SA. Human-robot collision detection and identification based on wrist and base force/torque sensors. In: *Proceedings of the IEEE international conference on robotics and automation*, Barcelona, 18–22 April 2005, pp.3796–3801. New York: IEEE.
8. Lumelsky VJ and Cheung E. Real-time collision avoidance in teleoperated whole-sensitive robot arm manipulators. *IEEE T Syst Man Cy* 1993; 23: 194–203.
9. Yamada Y, Shin K, Tsuchida N, et al A tactile sensor system for universal joint sections of manipulators. *IEEE T Robotic Autom* 1993; 9: 512–517.
10. Phan S, Fan Quek Z, Shah P, et al. Capacitive skin sensors for robot impact monitoring. In: *Proceedings of the international conference on intelligent robots and systems*, 25–30 September 2011, San Francisco, CA, pp.2992–2997. New York: IEEE.
11. Yamada Y, Hirasawa Y, Huang S, et al. Human-robot contact in the safeguarding space. *IEEE: ASME T Mech* 1997; 2: 230–236.
12. De Luca A and Mattone R. Sensorless robot collision detection and hybrid force/motion control. In: *Proceedings of the IEEE international conference on robotics and automation*, Barcelona, 18–22 April 2005, pp.999–1004. New York: IEEE.
13. De Luca A, Albu-Schaffer A, Haddadin S, et al. Collision detection and safe reaction with the DLR-III lightweight manipulator arm. In: *Proceedings of the international conference on intelligent robots and systems*, Beijing, China, 9–15 October 2006, pp.1623–1630. New York: IEEE.
14. Magrini E, Flacco F and De Luca A. Control of generalized contact motion and force in physical human-robot interaction. In: *Proceedings of the IEEE international conference on robotics and automation*, Seattle, WA, 26–30 May 2015, pp.2298–2304. New York: IEEE.
15. Lee S-D, Kim M-C and Song J-B. Sensorless collision detection for safe human-robot collaboration. In: *Proceedings of the international conference on intelligent robots and systems*, Hamburg, 28 September–2 October 2015, pp.2392–2397. New York: IEEE.
16. Lee S-D and Song J-B. Sensorless collision detection based on friction model for a robot manipulator. *Int J Precis Eng Man* 2016; 17: 11–17.
17. Axelsson P, Karlsson R and Norrlof M. Bayesian state estimation of a flexible industrial robot. *Control Eng Pract* 2012; 20: 1220–1228.
18. Axelsson P and Norrlof M. Method to estimate the position and orientation of a triaxial accelerometer mounted to an industrial manipulator. In: *Proceedings of the 10th international IFAC symposium on robot control*, 2012, http://users.isy.liu.se/en/rt/axelsson/presentations/SYROCO2012_accpose.pdf
19. Quigley M, Brewer R, Soundararaj SP, et al. Low-cost accelerometers for robotic manipulator perception. In: *Proceedings of the international conference on intelligent robots and systems*, Taipei, Taiwan, 18–22 October 2010, pp.6168–6174. New York: IEEE.
20. Roan P, Deshpande N, Wang Y, et al. Manipulator state estimation with low cost accelerometers and gyroscopes. In: *Proceedings of the international conference on intelligent robots and systems*, Vilamoura, 7–12 October 2012, pp.4822–4827. New York: IEEE.
21. De Luca A and Mattone R. Actuator fault detection and isolation using generalized momenta. In: *Proceedings of*

the IEEE international conference on robotics and automation, Taipei, Taiwan, 14–19 September 2003, pp.634–639. New York: IEEE.
22. Haddadin S, Albu-Schaffer A, De Luca A, et al. Collision detection and reaction: a contribution to safe physical human-robot interaction. In: *Proceedings of the international conference on intelligent robots and systems*, Nice, 22–26 September 2008, pp.3356–3363. New York: IEEE.
23. Monmasson E and Cirstea MN. FPGA design methodology for industrial control systems—a review. *IEEE T Ind Electron* 2007; 54: 1824–1842.
24. Lin Z, Peter S and Bruyninckx H. An open embedded hardware and software architecture applied to industrial robot control. In: *Proceedings of the IEEE international conference on mechatronics and automation*, Chengdu, China, 5–8 August 2012. New York: IEEE.
25. Yang C, Luo J, Pan Y, et al. Personalized variable gain control with tremor attenuation for robot teleoperation. *IEEE T Syst Man Cy: S* 2017; PP: 1–12.